JAERI-M
83-198

ATOMIC STRUCTURE CALCULATION OF ENERGY LEVELS AND OSCILLATOR STRENGTHS IN Ti ION, III

(3s-3p and 3p-3d Transitions in Ti XI)

November 1983

Keishi ISHII*

日本原子力研究所
Japan Atomic Energy Research Institute

JAERI-M レポートは，日本原子力研究所が不定期に公刊している研究報告書です。
入手の問合わせは，日本原子力研究所技術情報部情報資料課（〒319—11 茨城県那珂郡東海村）あて，お申しこしください。なお，このほかに財団法人原子力弘済会資料センター（〒319-11 茨城県那珂郡東海村日本原子力研究所内）で複写による実費頒布をおこなっております。

JAERI-M reports are issued irregularly.
Inquiries about availability of the reports should be addressed to Information Section, Division of Technical Information, Japan Atomic Energy Research Institute, Tokai-mura, Naka-gun, Ibaraki-ken 319-11, Japan.

編集兼発行　日本原子力研究所
印　　刷　山田軽印刷所

JAERI-M 83-198

Atomic Structure Calculation of Energy Levels and Oscillator Strengths in Ti Ion, III
(3s - 3p and 3p - 3d transitions in Ti XI)

Keishi ISHII*

(Received October 28 ,1983)

Energy levels and oscillator strengths were calculated for 3s-3p and 3p-3d transition arrays in Ti XI, isoelectronic to Mg I. The energy levels are obtained by the Slater-Condon theory of atomic structure, including explicitly the strong configuration interactions. The calculated wavelengths are presented for electric dipole transition with $gf \geqq 0.0001$. The calculated energy levels are given in diagrams, too. The theoretical spectra are also shown in graphical representation, where the gf is plotted as a function of the wavelength. The results are compared with experimental data, where available.

Keywords: Ti IX, Highly Ionized Atom, Wavelength, Energy Level, Oscillator Strength, Plasma Diagnostic, Cowan Program

---

This work is partly supported by a research contract of Japan Atomic Energy Research Institute with Kyoto University in fiscal year 1983. This work is herewith published for its value to scientific community.

* Department of Engineering Science, Kyoto University, Kyoto 606

Tiイオンのエネルギー準位と振動子強度の計算・Ⅲ
（Ti XIの3s－3pおよび3p－3d遷移）

石 井 慶 之*

（1983年10月28日受理）

核融合プラズマにおける不純物イオン問題解明のために必要とされる分光学的データに関する研究の一環として，Ti多価イオンの中でMgIと等電子系列であるTi XI の電子配置 $3s^k 3p^q 3d^r$ のエネルギー準位およびそれらの間の $\Delta n = 0$ 電気双極子遷移の振動子強度の理論計算を行った。計算の基礎は Hartree－XR波動関数と，Slater－Condon 理論に基づいた Cowan プログラムである。計算結果は表および図として与えた。文献調査による実験値は参考として表中に示した。

本報告は昭和58年度日本原子力研究所との協力研究の成果の一部である。

＊京都大学工学部物理工学教室　京都市左京区吉田本町

Contents

目　　次

§ 1. INTRODUCTION

Knowledge of atomic structure in multiply charged ions of metals is important in the interpretation of spectral data from high temperature plasma. The allowed $\Delta n=0$, $n=2-2$ transitions of $2s^2 2p^q - 2s2p^{q+1}$ and $2s2p^{q+1} - 2p^{q+2}$ types in highly ionized atoms have been widely studied. The energy level data have been compiled and published by Fawcett[1], and the data for oscillator strengths and the lifetimes are also available[2-5]. These data are now well established for the ions with $Z \leq 28$. The exception is the f-values for some transitions.

The data, however, on the energy levels of M-shell are not yet established. Little is known for oscillator strengths[2,6]. The wavelengths for $\Delta n=0$, $n=3-3$ transitions have been presented by Fawcett[7] again.

The Ti XI, a member of Mg I isoelectronic sequence ,have two electrons outside closed shell, which give rise to singlets and triplets. This spectrum has been studied first by Edlén[8] in 1936, and then by Fawcett & Peacock[9], by Fawcett[10], by Svensson & Ekberg[11] and by Ekberg[12]. Intercombination line, $3s^2\ {}^1S_0 - 3s3p\ {}^3P_1$, was not observed in the above works. Ekberg[12], however, extensively investigated Mg I-like spectra from K VIII to Ti XI, and tentatively identified two intercombination lines in Ca IX. He gave interpolated values of wavelengths of the intercombination lines of the other members along the isoelectronic sequence, using the data on Mg I, Al II, Si III, S V, Fe XV, and his data on Ca IX. Recently in 1982, Finkenthal *et al.*[13] studied the spectra from the TFR tokamak plasma, and measured the wavelength of the resonance intercombination as

569.3± 0.2 Å . This observed value was adopted in the present work to connect singlet and triplet system ,that is, to fix the floating uncertainty in the triplet systems.

Following the previous work on Ti IX[14] and Ti X[15] , the atomic structure calculation has been extended to Ti XI, using again the program developed by Cowan[16-18] . The energy levels have been obtained based on the Slater-Condon theory for $3s^2$, 3s3p, $3p^2$, 3s3d and 3p3d configurations, including explicitly the configuration interactions. The wavelengths and the weighted oscillator strengths (gf-values) have been calculated for 3s-3p and 3p-3d transitions. The results are given both in numerical tables and in the graphical representations. The calculated spectra are generated in such that the gf-value is plotted against wavelength. They will provide a helpful guidance for finding the missing lines, together with the numerical tables.

§ 2. METHOD OF CALCULATION

The method of calculation used in the present work is the same as in the previous ones[14,15] , and it is described in some detail there. The full explanation is given by Bromage[19] and Cowan[20] . Therefore only a short description is repeated here. The calculation consists of the following three steps:

(i) calculation of radial integrals, such as E_{av}, F^k , G^k , ζ_{nl} and R^k by the *ab initio* Hartree-XR wavefunctions,

(ii) optimization of the above integrals so as to minimize the discrepancy between the observed and calculated energy levels,

(iii) calculation of wavelengths and oscillator strengths by

569.3± 0.2 Å . This observed value was adopted in the present work to connect singlet and triplet system ,that is, to fix the floating uncertainty in the triplet systems.

Following the previous work on Ti IX[14] and Ti X[15] , the atomic structure calculation has been extended to Ti XI, using again the program developed by Cowan[16-18] . The energy levels have been obtained based on the Slater-Condon theory for $3s^2$, 3s3p, $3p^2$, 3s3d and 3p3d configurations, including explicitly the configuration interactions. The wavelengths and the weighted oscillator strengths (gf-values) have been calculated for 3s-3p and 3p-3d transitions. The results are given both in numerical tables and in the graphical representations. The calculated spectra are generated in such that the gf-value is plotted against wavelength. They will provide a helpful guidance for finding the missing lines, together with the numerical tables.

§ 2. METHOD OF CALCULATION

The method of calculation used in the present work is the same as in the previous ones[14,15] , and it is described in some detail there. The full explanation is given by Bromage[19] and Cowan[20] . Therefore only a short description is repeated here. The calculation consists of the following three steps:

(i) calculation of radial integrals, such as E_{av}, F^k , G^k , ζ_{nl} and R^k by the *ab initio* Hartree-XR wavefunctions,

(ii) optimization of the above integrals so as to minimize the discrepancy between the observed and calculated energy levels,

(iii) calculation of wavelengths and oscillator strengths by

adopting the scaled radial integrals obtained in the step (ii).

The steps (i) and (ii) were performed separately for the following two configuration groups according to the parity:

1st parity $3s^2$ (①), $3p^2$ (⑧) and 3s3d(⑫)

2nd parity 3s3p(①) and 3p3d(⑧)

The electric dipole radial integrals were also computed by the same Hartree-XR wavefunctions, and used in the step (iii) calculation.

§ 3. RESULTS

The first step calculation gives the *ab initio* values of the single configuration integrals and configuration interaction integrals as shown in the second column "HXR" of Tables 1 and 3. In the second step calculation, the optimization was reduced to manageable size by fixing ratio of F^k, G^k, ζ and R^k in each integrals[21-23], when necessary. The accuracy of the optimization was measured by a root mean square deviation (Δ) and/or a standard deviation (σ), defined as

$$\Delta=\left[\sum_i (E_{calc}(i)-E_{obs}(i))^2/(N_l-N_p)\right]^{1/2} \quad , \tag{1}$$

$$\sigma=\left[\sum_i (E_{calc}(i)-E_{obs}(i))^2/N_l\right]^{1/2} \quad , \tag{2}$$

where $E_{calc}(i)$ and $E_{obs}(i)$ are i-th calculated and observed levels, respectively, N_ℓ is the number of observed energy levels and N_p is the number of adjustable parameters. The following five

adopting the scaled radial integrals obtained in the step (ii).

The steps (i) and (ii) were performed separately for the following two configuration groups according to the parity:

1st parity $3s^2$ (𝔄), $3p^2$ (𝔅) and 3s3d(ℭ)

2nd parity 3s3p(𝔄) and 3p3d(𝔅)

The electric dipole radial integrals were also computed by the same Hartree-XR wavefunctions, and used in the step (iii) calculation.

§ 3. RESULTS

The first step calculation gives the *ab initio* values of the single configuration integrals and configuration interaction integrals as shown in the second column "HXR" of Tables 1 and 3. In the second step calculation, the optimization was reduced to manageable size by fixing ratio of F^k, G^k, ζ and R^k in each integrals[21-23], when necessary. The accuracy of the optimization was measured by a root mean square deviation (Δ) and/or a standard deviation (σ), defined as

$$\Delta=\left[\sum_i (E_{calc}(i)-E_{obs}(i))^2/(N_l-N_p)\right]^{1/2} \quad , \tag{1}$$

$$\sigma=\left[\sum_i (E_{calc}(i)-E_{obs}(i))^2/N_l\right]^{1/2} \quad , \tag{2}$$

where $E_{calc}(i)$ and $E_{obs}(i)$ are i-th calculated and observed levels, respectively, N_ℓ is the number of observed energy levels and N_p is the number of adjustable parameters. The following five

kinds of free parameters were used in the optimization:

one average energy E_{av}
one scale factor for F^k
one scale factor for G^k
one scale factor for ζ
two scale factors for R^k.

The reduced electric dipole radial integrals obtained from the same *ab initio* HXR wavefunctions were utilized in the step (iii) calculation combined with the second step results. In the following Tables and Figures, we closely maintain the format of our previous work on Ti IX[14] and Ti X[15].

3.1. *Configurations* $3s^2$ (𝔄), $3p^2$ (𝔅) *and* 3s3d(ℭ) *of the first parity*

Two levels of $^1S_0$ and $^1D_2$ in $3p^2$ configuration, and one level $^1D_2$ in 3s3d are known[10,12]. The floating uncertainty (x) of the triplet system was fixed from the observed wavelength of the resonance intercombination[13]. The energy of $3p^2\ ^1D_2$ of $408.821 \times 10^3\ cm^{-1}$ is given in Table V of Ekberg[12], and that of $3p^2\ ^1S_0$ of $482.84 \times 10^3\ cm^{-1}$ is derived from the observed wavelength of 446.69 Å for $3s3p\ ^1P_1 - 3p^2\ ^1S_0$ transition[7]. The least-squares optimization cannot be satisfactory, when the above two levels are included at the same time. Therefore, one of them had to be excluded. We have omitted the $^1S_0$ level, because isoelectronic regularity of the energy level of $^1S_0$ from K VIII to Fe XV is found poorer than that of $^1D_2$. Three singlet and six

triplet levels corrected by taking $x=1.82\times10^{3}\,cm^{-1}$, were adopted in the present calculation. In the least-squares optimization, the single configuration parameters were adjusted first, while R^k integrals were fixed. Then R^k integrals were adjusted by keeping the single configuration parameters fixed. This procedure was repeated several times. The fitted parameter values are given in the column "Fitted", and the ratio of "Fitted" to "HXR". The *rms* deviation Δ is $0.014\times10^{3}\,cm^{-1}$, which gives 0.001% of total energy range of the configurations (𝒶+𝒷+𝒸).

The calculated and observed energy levels are listed in Table 2 for the $3s^2$, $3p^2$ and 3s3d, together with their differences ("E(C-O)"), assuming again $x=1.82\times10^{3}\,cm^{-1}$. The agreement is satisfactory. One exception is $3p^2\ {}^1S$, which is excluded in the optimization calculation. The level designation and its percentage compositions in LS-basis are also given. The corresponding energy level diagram is shown in Fig.1 for $3p^2$ and 3s3d configurations. The percentage compositions are listed from the largest two contributions in the same configuration and one from the other when over about 10%. The average LS-purity is as high as 94%. Hence, the level designation in the column "Term" is given in LS-coupling notation by the most significant component. A pair of levels $3p^2\ {}^1D_2$ and $3s3d\ {}^1D_2$ are considerably perturbed with strong mutual configuration interaction: $3p^2\ {}^2D$ has a 19% $3s3d\ {}^2D$ character. One can notice that the appreciable mixing occurs between ${}^3P_2$ and ${}^1D_2$ levels in $3p^2$. This singlet-triplet mixing gives appreciable oscillator strength for some intercombination transitions, which is strictly forbidden in pure LS-coupling.

3.2. *Configurations* 3s3p(𝔄) *and* 3p3d(𝔅) *of the second parity*

The least-squares optimization was performed for the 3s3p(𝔄) and 3p3d(𝔅) configurations, in which one singlet and eight triplet levels were included. The energy of the triplet levels were fixed relative to ground level, based on the observed intercombination[13], $3s^2\ {}^1S_0 - 3s3p\ {}^3P_1$. The floating uncertainty x was estimated as $1.82\times10^3\,cm^{-1}$. The *rms* deviation Δ of $0.123\times10^3\,cm^{-1}$ was achieved, which yield 0.020% of total energy level spread of configurations 𝔄 and 𝔅. The Hartree-XR and fitted parameter values are given in Table 3, together with their ratios. The calculated energy levels are given in Table 4, along with the principal percentage compositions in LS-coupling basis. The observed energy levels are also included for comparison, with their difference with the calculated one. The average LS-purity of 3s3p configuration is close to 100%. It should be noted here that the ${}^3P_1$ level has only a 0.2% ${}^1P_1$ character and consiquently the oscillator strength for $3s^2\ {}^1S_0 - 3s3p\ {}^3P_1$ transition is small as described in 3.3. Energy level diagram for 3s3p configuration is displayed in Fig.2.

In 3p3d configuration, two levels, 726.12 and 731.77, are strongly mixed one another. Although their LS-purity is a little higher than 50%, they are labeled as ${}^3D_2$ and ${}^3P_2$, respectively, form their most significant composition. There is a considerable mixing between ${}^3F_2$ and ${}^1D_2$ levels. This indicates that some spin-forbidden transitions from 3p3d to $(3s3d + 3p^2)$ gain appreciable oscillator strenghth, as will be described in 3.3. The calculated energy levels are displayed graphically in Fig.3.

3.3. *Wavelengths and Oscillator Strengths*

The reduced electric dipole radial integrals (Table 10) were obtained from the *ab initio* Hatree-XR wavefunction, and used in the third step calculation without scaling. The calculated wavelengths and the *gf*-values for $3s^2$ - 3s3p, $3s^2$ - 3p3d, 3s3p - $3p^2$ and 3s3p - 3s3d transition arrays are listed in Table 5, and those for 3s3p - 3s3d in Table 6, and $3p^2$ - 3p3d in Table 7, respectively. In Tables 5-7, the observed wavelengths are included for comparison, with the difference between the calculated and observed ones. The agreement of the calculated wavelengths with the observed ones is excellent. In Table 5, the calculated *gf*-values are also given, together with the values derived by Wiese and Fuhr[6] for comparison. The agreement is again good. Table 5 shows that the difference between the calculated and observed wavelengths is less than 0.1 Å for all the components of ^3P - ^3P and ^1P - ^1D in 3s3p - $3p^2$ transition. Therefore, the accuracy of the calculated wavelength for two intercombinations, $^3P_2$ - $^1D_2$ and $^3P_1$ - $^1D_2$, is reliable in the same degree as for the allowed transitions described above. These two lines have fairly large *gf*-value, so that they are likely to be observed at the predicted position within ± 0.1Å . For a line of $^1P_1$ - $^1S_0$ in 3s3p - $3p^2$ transition, the calculated wavelength differs from the observed one[7] by 8.39Å . This is exceptionally large compared with other members, because of the fact that $3p^2$ $^1S_0$ was excluded in the least squares optimization of the energy level calculation. As is noted in 3.2, the isoelectronic regularity in energy level of $3p^2$ $^1S_0$ is poorer than that of

other levels. Therefore, we conclude that there are two ways, whereby the identification is completed in this spectrum. First, this line should be examined again along the isoelectronic sequence. Next, if this transition is confirmed as it is now, the model used in the present calculation has to be modified.

The total number of possible electric dipole transitions among the configurations considered in the present work is shown in Table 8, arranged in decreasing order of wavelength. The listed transitions are limited for $gf \geqq 0.0001$. Three lines at 316.987 Å , 259.448 Å and 124.940 Å given in Table 2 of ref.11 are tentatively assigned, and shown with a dagger. The theoretical spectrum was generated from Table 8, and displayed in Fig.4, where the gf-values are plotted in a logarithmic scale as a function of wavelength. Twelve lines above 560 Å and one line below 240 Å were excluded. Two line rich regions, 306 - 328 Å and 424 - 444 Å are shown in Figures 5 and 6, respectively, with wavelength scale being expanded ten times as large as in Fig.4. Three Figures 5-7 provide a helpful guidance for identification of missing lines by direct comparison with a recorded spectrogram.

Comparison of the present gf-value with that of Wiese and Fuhr, listed in Table 5, is graphically displyed in Fig.7, where $\log(gf)_{WF} - \log(gf)_{Present}$ is plotted against $\log(gf)_{Present}$. The $\log(gf)_{WF}$ is the data of Wiese and Fuhr[6] . The are between two dashed lines shows agreement within ± 20%.

In Table 9, the calculated lifetimes for the excited configurations are tabulated. Most of the levels have lifetimes of the order of 0.01 nsec, while $3s3p\ ^3P_{0,2}$ are metastable. It

should be noted that 3s3p $^3P_1$ level has such a long lifetime of 104 nsec that this level is collisionally destroyed before it decays by radiative transition. This indicates that the resonance intercombination is hardly observed from the ordinary light source, where electron density is usually high. Table 9 may provide practical help for the future beam-foil lifetime measurement.

§ 4. DISCUSSION

The average LS-purity of the first excited configuration of 3s3p is close to 100%, as shown in Table 4. On the other hand, the LS-purity of the levels of 3p3d configuration ranges from 55% to 100%, and the average is 76%. The purity varies from level to level in one configuration, and a few level has heavy admixtures from another configuration. In $3p^2$ configuration, the LS-purity of $^3P_0$ and $^3P_1$ is almost 100%, while that of $^3P_2$ is 91%. This gives the reasonable explanation for a difference of the gf-values between the present intermediate calculation and "LS-multiplet" one[6], for 3s3p ^3P_J – $3p^2$ $^3P_{J'}$ transition in Table 5. The gf-value of the lines originating from J=0 and 2 shows good agreement, while that from J=1 does not. That is, a part of the oscillator strength for the latter transition is transfered to other transitions.

In Tables 6 and 7, one can notice that several lines with fairly large gf-value are not yet observed. Some of them are thus expected to be found in the recorded spectrogram. The present calculation, especially the calculated spectra shown in Figures 4-6, may provide helpful guidance for finding these missing

should be noted that 3s3p $^3P_1$ level has such a long lifetime of 104 nsec that this level is collisionally destroyed before it decays by radiative transition. This indicates that the resonance intercombination is hardly observed from the ordinary light source, where electron density is usually high. Table 9 may provide practical help for the future beam-foil lifetime measurement.

§ 4. DISCUSSION

The average LS-purity of the first excited configuration of 3s3p is close to 100%, as shown in Table 4. On the other hand, the LS-purity of the levels of 3p3d configuration ranges from 55% to 100%, and the average is 76%. The purity varies from level to level in one configuration, and a few level has heavy admixtures from another configuration. In $3p^2$ configuration, the LS-purity of $^3P_0$ and $^3P_1$ is almost 100%, while that of $^3P_2$ is 91%. This gives the reasonable explanation for a difference of the gf-values between the present intermediate calculation and "LS-multiplet" one[6], for 3s3p ^3P_J - $3p^2$ $^3P_{J'}$ transition in Table 5. The gf-value of the lines originating from J=0 and 2 shows good agreement, while that from J=1 does not. That is, a part of the oscillator strength for the latter transition is transfered to other transitions.

In Tables 6 and 7, one can notice that several lines with fairly large gf-value are not yet observed. Some of them are thus expected to be found in the recorded spectrogram. The present calculation, especially the calculated spectra shown in Figures 4-6, may provide helpful guidance for finding these missing

lines, although in many cases the apparent line intensity is dependent on conditions of a light source.

The radial energy integrals were adjusted from their *ab initio* Hartree-XR values, while the radial electric dipole integrals were not. Therefore, the *gf*-values of transition between levels, of which at least one is subject to strong configuration interaction, are less accurate. However, the relative *gf*-values are fairly reliable, because the dipole integrals have a very little influence on them. Wiese and Fuhr[6] noted that the *gf*-values in their table need to be replaced by intermediate coupling data. The present calculation meets to this need. The transition probability situation in Ti XI is thus improved. The absolute *gf*-values can be determined only after the lifetimes are measured. In this context, Table 9 may be helpful for practical purpose of lifetime measurement.

The compilation of spectroscopic data on Ti V - Ti XXII has recently been updated by Mori[24]. The energy levels, wavelengths, oscillator strengths and/or transition probabilities are given both in numerical tables and in Grotorian diagram. The relevant source references are also attached. A series of our works on Ti IX[14], Ti X[15] and Ti XI of the present can be partly a extension of ref.24. In this report we present not only comparison of the calculated and the observed data with some discussions, but also the whole possible energy levels and transitions including predicted wavelengths and *gf*-values. Thus we conclude that those transitions in ref.24 which are conflicting with the present calculation need to be checked further, in order to obtain complete knowledge of atomic

structure of Ti ions.

The author would like to express his sincere thanks to Dr. Robert D. Cowan for making his programs available, and to Dr. Jan O. Ekberg for his kindest help to make MT copies of the programs and for his valuable discussions regarding the application of the program to the present work. He owes his thanks to Drs. K. Ozawa, Y. Nakai and T. Shirai of Japan Atomic Energy Research Institute for their valuable comments and for their arrangement of the publication of the report. The present calculation have been carried out by use of the computer FACOM M-380 at the Data Processing Center of Kyoto University.

REFERENCES

1) B.C. Fawcett: "Wavelengths and classifications of emission lines due to $2s^2 2p^n - 2s2p^{n+1}$ and $2s2p^{n+1} - 2p^{n+2}$ transitions, $Z \leqq 28$", Atomic Data and Nuclear Data Tables 16 (1975) 135-164.

2) M.W. Smith and W.L. Wiese: "Graphical representations of systematic trends of atomic oscillator strengths along isoelectronic sequences and new oscillator strengths derived by interpolation", Astrophys. J. Suppl. Ser. 196 (1971) 103-192.

3) K. Ishii: "Systematic trends of oscillator strengths and lifetimes for $\Delta n=0$, n=2-2 transitions in multiply charged ions along isoelectronic sequence", U.S.-Japan Seminar on Plasma Spectroscopy, Kyoto (1979) p.54.

4) B.C. Fawcett: "Theoretical oscillator strengths for $2s^2 2p^n - 2s2p^{n+1}$ and $2s2p^{n+1} - 2p^{n+2}$ transitions and for $2s^2 2p^n$ "forbidden" transitions, Be I, B I, C I, N I, O I series, $Z \leqq 26$", Atomic Data and Nuclear Data Tables 22 (1978) 473-489.

5) K.T. Cheng, Y.-K. Kim and J.P. Desclaux: "Electric dipole, quadrupole, and magnetic dipole transition probabilities of ions isoelectronic to the first-row atoms, Li through F", Atomic Data and Nuclear Data Tables 24 (1979) 111-189.

6) W.L. Wiese and J.R. Fuhr: "Atomic transition probabilities for scandium and titanium (a critical compilation of allowed lines)", J. Phys. Chem. Ref. Data 4 (1975) 263-352.

7) B.C. Fawcett: "Wavelengths and classifications of emission lines due to $3s^2 3p^n - 3s3p^{n+1}$ $3s3p^{n+1} - 3s^2 3p^{n-1}3d$ and other n=3-3

transitions", Report ARU-R4, Culham laboratory, UK (1971).

8) B. Edlén: "Mg I-ähnlich Spektren der Elementen Titan bis Cobalt, Ti XI, V XII, Cr XIII, Mn XIV, Fe XV and Co XVI", Z. Physik **103** (1936) 536-541.

9) B.C. Fawcett and N.J. Peacock: "Highly ionized spectra of the transiton elements", Proc. Phys. Soc. **91** (1967) 973-975.

10) B.C. Fawcett: "Classification of the lower lying energy levels of highly ionized transition elements", J. Phys. **B3** (1970) 1732-1741.

11) L.A . Svensson and J.O. Ekberg: "The titanium vacuum-spark spectrum from 50 to 425 A", Arkiv Fysik **40** (1969) 145-164.

12) J.O. Ekberg: "Analysis of the Mg-I like spectra K VIII, Ca IX, Sc X and Ti XI", Physica Scripta **4** (1971) 101-109.

13) M. Finkenthal, R.E. Bell and H.W. Moos: "Intercombination lines in Mg I-like Ti XI, V XII, Cr XIII and Fe XV spectra obtained from tokamak plasma", Phys. Lett. **88A** (1982) 165-168.

14) K. Ishii: "Atomic structure calculation of energy levels and oscillator strengths in Ti ion. (I. 3s-3p and 3p-3d transitions in Ti IX.)", JAERI-M 83-155 (Report of Japan Atomic Energy Research Institute, 1983).

15) K. Ishii: "Atomic structure calculation of energy levels and oscillator strengths in Ti ion. (II. 3s-3p and 3p-3d transitions in Ti X.)", JAERI-M 83-164 (Report of Japan Atomic Energy Research Institute, 1983).

16) R.D. Cowan: "Atomic self-consistent-field calculations using statistical approximations for exchange and correlation", Phys. Rev. **163** (1967) 54-61.

17) R.D. Cowan and D.C. Griffin: "Approximate relativistic corrections to atomic radial wavefunctions", J. Opt. Soc. Am. **66** (1976) 1010-1014.

18) R.D. Cowan: "Theoretical calculation of atomic spectra using digital computers", J. Opt. Soc. Am. **58** (1968) 808-818, and "Theoretical study of $p^m - p^{m-1}\ell$ spectra", *ibid.* **58** (1968) 924-933.

19) G.E. Bromage: "The Cowan-Zealot-Suite of computer programs for atomic structure", Report AL-R-3, Appleton Laboratory, UK (1978).

20) R.D. Cowan: *The Theory of Atomic Structure and Spectra* (Univ. Calif. Press, Berkley, 1981).

21) G.E. Bromage, R.D. Cowan and B.C. Fawcett: "Energy levels and oscillator strengths for $3s^2 3p^n - 3s^2 3p^{n-1} 3d$ transitions of Fe X and Fe XI", Physica Scripta **15** (1977) 177-182.

22) G.E. Bromage, R.D. Cowan and B.C. Fawcett: "Atomic structure calculations involving optimization of radial integrals: Energy levels and oscillator strengths for Fe XII and Fe XIII 3p-3d and 3s-3p transitions", Mon. Not. R. astr. Soc. **183** (1978) 19-28.

23) G.E. Bromage: "Atomic structure calculations: Energy levels and oscillator strengths for 3s-3p and 3p-3d transitions in nickel XII to XV and vanadium VII to X spectra", Astron. Astrophys. Suppl. Ser. **41** (1980) 79-83.

24) K. Mori: "Grotorian Diagrams for highly ionized titanium Ti V - Ti XXII", JAERI-M 82-078 (Report of Japan Atomic Energy Research Institute, 1982).

ADDENDA

Present calculation of Ti XI was carried out as an extension of the previous work on Ti IX and Ti X. After the completion of the present work, Fawcett[1,2] published the same calculation on Ti XI. While we were concentrated on Ti, he presented systematic calculations of Al-like ions from Cl V to Ni XVI and Mg-like ions from S V to Ni XVII. The present results are in agreement with ref.[2]. However, when compared with the observed data, the present results show better agreement. We present here the wavelengths and *gf*-values for forbidden lines in addition to that for allowed ones. The graphical representations are also diaplayed.

[1] B.C. Fawcett: "Calculated oscillator strenghts and wavelengths for allowed transitions within the third shell for ions in the Al-like isoelectronic sequence between Cl V and Ni XVI", Atomic Data and Nuclear Data Tables 28 (1983) 557-578.

[2] B.C. Fawcett: "Calculated oscillator strenghts and wavelengths for allowed transitions within the third shell for ions in the Mg-like isoelectronic sequence between S V and Ni XVII", Atomic Data and Nuclear Data Tables 28 (1983) 579-596.

Table 1 Parameter values (in $10^3 cm^{-1}$) for $3s^2$, $3p^2$ and 3s3d configurations in Ti XI. Ratio is defined as Fitted/HXR.

Parameters	Hartree-XR	Fitted	Ratio	C.I.
$E_{av}(3s^2)$	0.000	5.761	-----	
$E_{av}(3p^2)$	418.845	429.543	1.026	
$F^2(3p,3p)$	114.529	106.339	0.928	
$\zeta(3p)$	5.906	5.465	0.925	
$E_{av}(3s,3d)$	499.026	508.228	1.018	
$\zeta(3d)$	0.510	0.324	0.635	
$G^2(3s,3d)$	102.792	79.923	0.778	
$R^1(ss,pp)$	149.888	91.144	0.608	$3s^2 * 3p^2$
$R^1(pp,sd)$	137.304	121.144	0.882	$3p^2 * 3s3d$
Δ		0.014*		
σ		0.007		

*Number of free parameter is 7.

Table 2 Calculated and observed energy levels (in $10^3 cm^{-1}$) for $3s^2$, $3p^2$ and 3s3d configurations.

Conf	Term	J	E(calc)	E(obs)	E(C-O)*	Percentage Composition
$3s^2$	^1S	0	0.00	0.000	0.00	99%
$3p^2$	^3P	2	420.60	418.775+x[a]	0.00	91%, 7% ^1D
	^3P	1	414.05	412.226+x[a]	0.00	100%
	^3P	0	410.54	408.712+x[a]	0.01	99%
	^1D	2	408.82	408.821[a]	0.00	72%, 9% ^3P, 19% 3s3d ^1D
	^1S	0	487.13	482.84 [b]	4.29†	98%
3s3d	^3D	3	500.56	498.728+x[a]	0.01	100%
	^3D	2	500.07	498.239+x[a]	0.01	100%
	^3D	1	499.75	497.918+x[a]	0.01	100%
	^1D	2	564.60	564.604[a]	0.00	79%, 21% $3p^2$ ^1D

*When assumed uncertainty x=1.82.
[a] Ekberg (1971), ref.12).
[b] Fawcett (1971), ref.7).
[c] Finkental *et al.* (1982), ref.13).
†See text.

Table 3 Parameter values (in $10^3 cm^{-1}$) for 3s3p and 3p3d configurations in Ti XI. Ratio is defined as Fitted/HXR.

Parameters	Hartree-XR	Fitted	Ratio	C.I.
E_{av}(3s3p)	188.448	202.381	1.074	
ζ(3p)	5.946	5.472	0.921	
G^1(3s,3p)	150.513	134.396	0.893	
E_{av}(3p3d)	710.766	722.457	1.016	
ζ(3p)	5.920	5.307	0.896	
ζ(3d)	0.510	0.372	0.730	
F^2(3p,3d)	114.431	120.939	1.057	
G^1(3p,3d)	131.324	129.496	0.986	
G^3(3p,3d)	85.476	84.286	0.986	
R^1(sp,pd)	137.576	110.061	0.800	3s3p * 3p3d
R^2(sp,pd)	104.998	84.000	0.800	3s3p * 3p3d
Δ		0.123*		
σ		0.041		

* Number of free parameter is 7.

Table 4 Calculated and observed energy levels (in $10^3 cm^{-1}$) for 3s3p and 3p3d configurations in Ti XI.

Conf	Term	J	E(calc)	E(obs)	E(C-O)*	% Composition
3s3p	^{3}P	2	181.27	179.473+x^a	0.02	100%
	^{3}P	1	175.65	173.827+x^a	0.00	100%
				175.65[c]	0.00	
	^{3}P	0	173.09	171.274+x^a	0.00	100%
	^{1}P	1	258.97	258.973[a]	0.00	98%
3p3d	^{3}F	4	691.81	690.06+x^b	-0.07	100%
	^{3}F	3	687.59	685.66+x^b	0.11	100%
	^{3}F	2	683.76	682.00+x^b	-0.06	89%, 11% ^{1}D
	^{3}D	3	730.43	728.64+x^b	-0.03	100%
	^{3}D	2	726.17	724.35+x^b	0.00	55%, 45% ^{3}P
	^{3}D	1	726.21			82%, 18% ^{3}P
	^{3}P	2	731.77			55%, 45% ^{3}D
	^{3}P	1	732.07			82%, 18% ^{3}D
	^{3}P	0	732.14			100%
	^{1}F	3	794.66			100%
	^{1}D	2	692.51			89%, 10% ^{3}F
	^{1}P	1	800.30			98%

* When assumed uncertainty x=1.82.
[a,b,c] See footnote in Table 2.

Table 5 Calculated and observed wavelengths for $3s^2$ - 3s3p, $3s^2$ - 3p3d, 3s3p - $3p^2$ and 3s3p - 3s3d transition arrays in Ti XI, with calculated weighted oscillator strengths.

Transition			Wavelength (in A)				
Conf	Term	J-J	Calc	Obs	C-O	gf	gf^*
$3s^2$ -3s3p	$^1S-^1P$	0-1	386.140	386.140[a]	0.00	1.0245	0.96
	$^1S-^3P$	0-1	569.325	569.3[c]	0.00	0.0014	
$3s^2$ -3p3d	$^1S-^1P$	0-1	124.953	124.940[d†]	0.013	0.0085	
3s3p-$3p^2$	$^3P-^3P$	2-2	417.837	417.85[b]	-0.01	1.1458	1.30
	$^3P-^3P$	1-2	408.240	408.28[b]	-0.04	0.3787	0.42
	$^3P-^3P$	2-1	429.594	429.60[b]	-0.01	0.4098	0.41
	$^3P-^3P$	1-1	419.456	419.45[b]	0.01	0.2519	0.25
	$^3P-^3P$	0-1	415.012	415.07[b]	-0.06	0.3402	0.34
	$^3P-^3P$	1-0	425.723	425.74[b]	-0.02	0.3305	0.33
	$^1P-^1D$	1-2	667.342	667.12[b]	0.12	0.3284	0.39
	$^1P-^1S$	1-0	438.300	446.69[b†]	(8.39)	0.3334	0.39
	$^3P-^1D$	2-2	439.466			0.1134	
	$^3P-^1D$	1-2	428.862			0.0521	
	$^3P-^1S$	1-0	321.047			0.0012	
	$^1P-^3P$	1-2	618.709			0.0412	
	$^1P-^3P$	1-1	644.840			0.0003	
	$^1P-^3P$	1-0	659.771			0.0007	
3s3p-3s3d	$^3P-^3D$	2-3	313.197	313.229[a]	-0.032	1.6558	1.75
	$^3P-^3D$	2-2	313.676	313.710[a]	-0.034	0.2958	0.32
	$^3P-^3D$	1-2	308.236	308.250[a]	-0.014	0.9010	0.96
	$^3P-^3D$	2-1	313.993	314.03 *		0.0197	0.022
	$^3P-^3D$	1-1	308.543	308.568[a]	-0.025	0.3001	0.33
	$^3P-^3D$	0-1	306.132	306.144[a]	-0.012	0.4041	0.43
	$^1P-^1D$	1-2	327.191	327.192[a]	-0.001	2.3913	2.40
	$^1P-^3D$	1-2	414.767			0.0009	
	$^1P-^3D$	1-1	415.322			0.0005	
	$^3P-^1D$	2-2	260.870			0.0002	
	$^3P-^1D$	1-2	257.096			0.0043	

[a] Ekberg (1971), ref.12). [c] Finkenthal *et al.* (1971), ref.13).
[b] Fawcett (1971), ref.7). [d] Svensson and Ekberg (1969), ref.11).
* Wiese and Fuhr (1975), ref.6).
† see text.

Table 6 Calculated and observed wavelengths for 3s3d - 3p3d transition in Ti XI, with calculated weighted oscillator strengths.

Transition			Wavelength (in A)			
Conf-Conf	Term-Term	J-J	Calc	Obs	C-O	gf
3s3d-3p3d	$^3D-^3F$	3-4	522.877	522.66[b]	0.22	1.3041
	$^3D-^3F$	3-3	534.673			0.1470
	$^3D-^3F$	2-3	533.282	533.55[b]	-0.27	0.8460
	$^3D-^3F$	3-2	545.847			0.0025
	$^3D-^3F$	2-2	544.397			0.1165
	$^3D-^3F$	1-2	543.444	543.23[b]	0.21	0.5050
	$^3D-^3D$	3-3	435.033	434.94[b]	0.09	1.0364
	$^3D-^3D$	2-3	434.112			0.1818
	$^3D-^3D$	3-2	443.236			0.7606
	$^3D-^3D$	2-2	442.280			0.0897
	$^3D-^3D$	1-2	441.650			0.0539
	$^3D-^3D$	2-1	442.217			0.3629
	$^3D-^3D$	1-1	441.588			0.1625
	$^3D-^3P$	3-2	432.516			0.1851
	$^3D-^3P$	2-2	431.606			0.6422
	$^3D-^3P$	1-2	431.006			0.1155
	$^3D-^3P$	2-1	431.038			0.2080
	$^3D-^3P$	1-1	430.440			0.3790
	$^3D-^3P$	1-0	430.307			0.2000
	$^1D-^1F$	2-3	434.687			2.9565
	$^1D-^1D$	2-2	781.813			0.1331
	$^1D-^1P$	2-1	424.282			0.8690
	$^1D-^3F$	2-3	813.105			0.0013
	$^1D-^3F$	2-2	839.230			0.0143
	$^1D-^3D$	2-3	603.054			0.0011
	$^1D-^3D$	2-2	618.932			0.0008
	$^1D-^3D$	2-1	618.809			0.0016
	$^1D-^3P$	2-2	598.229			0.0001
	$^3D-^1F$	3-3	340.026			0.0026
	$^3D-^1F$	2-3	339.462			0.0007
	$^3D-^1D$	3-2	520.962			0.0086
	$^3D-^1D$	2-2	519.641			0.0125
	$^3D-^1D$	1-2	518.772			0.0604
	$^3D-^1P$	2-1	333.083			0.0014
	$^3D-^1P$	1-1	332.726			0.0004

[b] Fawcett (1971), ref.7).

Table 7 Calculated and observed wavelengths for $3p^2$ - 3p3d transition in Ti XI, with calculated weighted oscillator strengths.

Transition			Wavelength (in A)			
Conf-Conf	Term-Term	J-J	Calc	Obs	C-O	gf
$3p^2$ -3p3d	$^3P-^3F$	2-3	374.545			0.0051
	$^3P-^3F$	2-2	379.994			0.0059
	$^3P-^3F$	1-2	370.766			0.0009
	$^3P-^3D$	2-3	322.760	322.75[b]	0.21	2.3410
	$^3P-^3D$	2-2	327.253			0.0225
	$^3P-^3D$	1-2	320.386			1.5603
	$^3P-^3D$	2-1	327.219			0.0046
	$^3P-^3D$	1-1	320.353			0.1978
	$^3P-^3D$	0-1	316.791			0.8695
	$^3P-^3P$	2-2	321.372			1.2609
	$^3P-^3P$	1-2	314.747			0.1569
	$^3P-^3P$	2-1	321.057			0.2992
	$^3P-^3P$	1-1	314.445			0.4655
	$^3P-^3P$	0-1	311.013			0.0135
	$^3P-^3P$	1-0	314.374			0.2472
	$^1D-^1F$	2-3	259.178			1.2829
	$^1D-^1D$	2-2	352.495			1.0810
	$^1D-^1P$	2-1	255.443			0.0072
	$^1S-^1P$	0-1	319.315			1.0351
	$^3P-^1F$	2-3	267.340			0.1573
	$^3P-^1D$	2-2	367.764			0.0865
	$^3P-^1D$	1-2	359.115			0.0071
	$^3P-^1P$	2-1	263.367			0.0010
	$^3P-^1P$	1-1	258.901			0.0004
	$^3P-^1P$	0-1	256.570			0.0032
	$^1D-^3F$	2-3	358.719			0.0029
	$^1D-^3F$	2-2	363.715			0.1295
	$^1D-^3D$	2-3	310.939			0.2912
	$^1D-^3D$	2-2	315.107			0.0017
	$^1D-^3D$	2-1	315.075			0.0003
	$^1S-^3D$	0-1	418.272			0.0011
	$^1D-^3P$	2-2	309.651			0.1049
	$^1D-^3P$	2-1	309.358			0.0314

[b] Fawcett (1971), ref.7).

Table 8 Calculated wavelengths for transitions between ($3s^2$ + $3p^2$ + 3s3d) and (3s3p + 3p3d) configurations with gf-value. Arranged in order of decreasing wavelength.

No	Transitin: Energy(10^3 cm^{-1})	Conf	Term	J-J	Wavelength(A): Calc	Obs	gf
1	564.604-683.761	3s3d-3p3d	$^1D-^3F$	2-2	839.230		0.0143
2	564.604-687.590	3s3d-3p3d	$^1D-^3F$	2-3	813.105		0.0013
3	564.604-692.512	3s3d-3p3d	$^1D-^1D$	2-2	781.813		0.1331
4	258.972-408.820	3s3p-$3p^2$	$^1P-^1D$	1-2	667.342	667.12[b]	0.3284
5	258.972-410.540	3s3p-$3p^2$	$^1P-^3P$	1-0	659.771		0.0007
6	258.972-414.049	3s3p-$3p^2$	$^1P-^3P$	1-1	644.840		0.0003
7	564.604-726.173	3s3d-3p3d	$^1D-^3D$	2-2	618.932		0.0008
8	564.604-726.205	3s3d-3p3d	$^1D-^3D$	2-1	618.809		0.0016
9	258.972-420.599	3s3p-$3p^2$	$^1P-^3P$	1-2	618.709		0.0412
10	564.604-730.427	3s3d-3p3d	$^1D-^3D$	2-3	603.054		0.0011
11	564.604-731.764	3s3d-3p3d	$^1D-^3P$	2-2	598.229		0.0001
12	-0.001-175.645	$3s^2$ -3s3p	$^1S-^3P$	0-1	569.325	569.3[c]	0.0014
13	500.559-683.761	3s3d-3p3d	$^3D-^3F$	3-2	545.847		0.0025
14	500.072-683.761	3s3d-3p3d	$^3D-^3F$	2-2	544.397		0.1165
15	499.749-683.761	3s3d-3p3d	$^3D-^3F$	1-2	543.444	543.23[b]	0.5050
16	500.559-687.590	3s3d-3p3d	$^3D-^3F$	3-3	534.673		0.1470
17	500.072-687.590	3s3d-3p3d	$^3D-^3F$	2-3	533.282	533.55[b]	0.8460
18	500.559-691.809	3s3d-3p3d	$^3D-^3F$	3-4	522.877	522.66[b]	1.3041
19	500.559-692.512	3s3d-3p3d	$^3D-^1D$	3-2	520.962		0.0086
20	500.072-692.512	3s3d-3p3d	$^3D-^1D$	2-2	519.641		0.0125
21	499.749-692.512	3s3d-3p3d	$^3D-^1D$	1-2	518.772		0.0604
22	500.559-726.173	3s3d-3p3d	$^3D-^3D$	3-2	443.236		0.7606
23	500.072-726.173	3s3d-3p3d	$^3D-^3D$	2-2	442.280		0.0897
24	500.072-726.205	3s3d-3p3d	$^3D-^3D$	2-1	442.217		0.3629
25	499.749-726.173	3s3d-3p3d	$^3D-^3D$	1-2	441.650		0.0539
26	499.749-726.205	3s3d-3p3d	$^3D-^3D$	1-1	441.588		0.1625
27	181.271-408.820	3s3p-$3p^2$	$^3P-^1D$	2-2	439.466		0.1134
28	258.972-487.126	3s3p-$3p^2$	$^1P-^1S$	1-0	438.300	446.69[b†]	0.3334
29	500.559-730.427	3s3d-3p3d	$^3D-^3D$	3-3	435.033	434.94[b]	1.0364
30	564.604-794.655	3s3d-3p3d	$^1D-^1F$	2-3	434.687		2.9565
31	500.072-730.427	3s3d-3p3d	$^3D-^3D$	2-3	434.112		0.1818
32	500.559-731.764	3s3d-3p3d	$^3D-^3P$	3-2	432.516		0.1851
33	500.072-731.764	3s3d-3p3d	$^3D-^3P$	2-2	431.606		0.6422
34	500.072-732.070	3s3d-3p3d	$^3D-^3P$	2-1	431.038		0.2080
35	499.749-731.764	3s3d-3p3d	$^3D-^3P$	1-2	431.006		0.1155
36	499.749-732.070	3s3d-3p3d	$^3D-^3P$	1-1	430.440		0.3790
37	499.749-732.141	3s3d-3p3d	$^3D-^3P$	1-0	430.307		0.2000
38	181.271-414.049	3s3p-$3p^2$	$^3P-^3P$	2-1	429.594	429.60[b]	0.4098
39	175.645-408.820	3s3p-$3p^2$	$^3P-^1D$	1-2	428.862		0.0521
40	175.645-410.540	3s3p-$3p^2$	$^3P-^3P$	1-0	425.723	425.74[b]	0.3305

Table 8 *Continued*

41	564.604–800.297	3s3d–3p3d	^1D–^1P 2–1	424.282	0.8690
42	175.645–414.049	3s3p–3p^2	^3P–^3P 1–1	419.456 419.45[b]	0.2519
43	487.126–726.205	3p^2 –3p3d	^1S–^3D 0–1	418.272	0.0011
44	181.271–420.599	3s3p–3p^2	^3P–^3P 2–2	417.837 417.85[b]	1.1458
45	258.972–499.749	3s3p–3s3d	^1P–^3D 1–1	415.322	0.0005
46	173.093–414.049	3s3p–3p^2	^3P–^3P 0–1	415.012 415.07[b]	0.3402
47	258.972–500.072	3s3p–3s3d	^1P–^3D 1–2	414.767	0.0009
48	175.645–420.599	3s3p–3p^2	^3P–^3P 1–2	408.240 408.28[b]	0.3787
49	–0.001–258.972	3s^2 –3s3p	^1S–^1P 0–1	386.140 386.140[a]	1.0245
50	420.599–683.761	3p^2 –3p3d	^3P–^3F 2–2	379.994	0.0059
51	420.599–687.590	3p^2 –3p3d	^3P–^3F 2–3	374.545	0.0051
52	414.049–683.761	3p^2 –3p3d	^3P–^3F 1–2	370.766	0.0009
53	420.599–692.512	3p^2 –3p3d	^3P–^1D 2–2	367.764	0.0865
54	408.820–683.761	3p^2 –3p3d	^1D–^3F 2–2	363.715	0.1295
55	414.049–692.512	3p^2 –3p3d	^3P–^1D 1–2	359.115	0.0071
56	408.820–687.590	3p^2 –3p3d	^1D–^3F 2–3	358.719	0.0029
57	408.820–692.512	3p^2 –3p3d	^1D–^1D 2–2	352.495	1.0810
58	500.559–794.655	3s3d–3p3d	^3D–^1F 3–3	340.026	0.0026
59	500.072–794.655	3s3d–3p3d	^3D–^1F 2–3	339.462	0.0007
60	500.072–800.297	3s3d–3p3d	^3D–^1P 2–1	333.083	0.0014
61	499.749–800.297	3s3d–3p3d	^3D–^1P 1–1	332.726	0.0004
62	420.599–726.173	3p^2 –3p3d	^3P–^3D 2–2	327.253	0.0225
63	420.599–726.205	3p^2 –3p3d	^3P–^3D 2–1	327.219	0.0046
64	258.972–564.604	3s3p–3s3d	^1P–^1D 1–2	327.191 327.192[a]	2.3913
65	420.599–730.427	3p^2 –3p3d	^3P–^3D 2–3	322.760 322.75[b]	2.3410
66	420.599–731.764	3p^2 –3p3d	^3P–^3P 2–2	321.372	1.2609
67	420.599–732.070	3p^2 –3p3d	^3P–^3P 2–1	321.057	0.2992
68	175.645–487.126	3s3p–3p^2	^3P–^1S 1–0	321.047	0.0012
69	414.049–726.173	3p^2 –3p3d	^3P–^3D 1–2	320.386	1.5603
70	414.049–726.205	3p^2 –3p3d	^3P–^3D 1–1	320.353	0.1978
71	487.126–800.297	3p^2 –3p3d	^1S–^1P 0–1	319.315	1.0351
72	410.540–726.205	3p^2 –3p3d	^3P–^3D 0–1	316.791 316.987[d†]	0.8695
73	408.820–726.173	3p^2 –3p3d	^1D–^3D 2–2	315.107	0.0017
74	408.820–726.205	3p^2 –3p3d	^1D–^3D 2–1	315.075	0.0003
75	414.049–731.764	3p^2 –3p3d	^3P–^3P 1–2	314.747	0.1569
76	414.049–732.070	3p^2 –3p3d	^3P–^3P 1–1	314.445	0.4655
77	414.049–732.141	3p^2 –3p3d	^3P–^3P 1–0	314.374	0.2472
78	181.271–499.749	3s3p–3s3d	^3P–^3D 2–1	313.993	0.0197
79	181.271–500.072	3s3p–3s3d	^3P–^3D 2–2	313.676 313.710[a]	0.2958
80	181.271–500.559	3s3p–3s3d	^3P–^3D 2–3	313.197 313.229[a]	1.6558
81	410.540–732.070	3p^2 –3p3d	^3P–^3P 0–1	311.013	0.0135
82	408.820–730.427	3p^2 –3p3d	^1D–^3D 2–3	310.939	0.2912
83	408.820–731.764	3p^2 –3p3d	^1D–^3P 2–2	309.651	0.1049
84	408.820–732.070	3p^2 –3p3d	^1D–^3P 2–1	309.358	0.0314
85	175.645–499.749	3s3p–3s3d	^3P–^3D 1–1	308.543 308.568[a]	0.3001
86	175.645–500.072	3s3p–3s3d	^3P–^3D 1–2	308.236 308.250[a]	0.9010
87	173.093–499.749	3s3p–3s3d	^3P–^3D 0–1	306.132 306.144[a]	0.4041
88	420.599–794.655	3p^2 –3p3d	^3P–^1F 2–3	267.340	0.1573
89	420.599–800.297	3p^2 –3p3d	^3P–^1P 2–1	263.367	0.0010
90	181.271–564.604	3s3p–3s3d	^3P–^1D 2–2	260.870	0.0002

Table 8 *Continued*

91	408.820–794.655	3s3d–3p3d ^{1}D–^{1}F 2–3	259.178	259.448[dt]	1.2829
92	414.049–800.297	3p^2 –3p3d ^{3}P–^{1}P 1–1	258.901		0.0004
93	175.645–564.604	3s3p–3s3d ^{3}P–^{1}D 1–2	257.096		0.0043
94	410.540–800.297	3p^2 –3p3d ^{3}P–^{1}P 0–1	256.570		0.0032
95	408.820–800.297	3p^2 –3p3d ^{1}D–^{1}P 2–1	255.443		0.0072
96	–0.001–800.297	3s^2 –3p3d ^{1}S–^{1}P 0–1	124.953	124.940[dt]	0.0085

[a] Ekberg (1971), ref.12).
[b] Fawcett (1971), ref.7).
[c] Finkenthal (1982), ref.13).
[d] Svensson and Ekberg (1969), ref.11).
[†] See text for detail.

Table 9 Calculated lifetimes (in nsec) for levels of the excited configurations in Ti XI.

Conf	Term	J	Energy	Lifetime*
$3p^2$	^3P	2	420.60	8.86(-2)
	^3P	1	414.05	7.99(-2)
	^3P	0	410.54	8.22(-2)
	^1D	2	408.82	4.66(-1)
	^1S	0	487.03	8.58(-2)
3s3d	^3D	3	500.56	6.22(-2)
	^3D	2	500.07	6.00(-2)
	^3D	1	499.75	5.87(-2)
	^1D	2	564.60	3.35(-2)
3s3p	^3P	2	181.27	----
	^3P	1	175.65	1.04(+2)
	^3P	0	173.09	----
	^1P	1	258.97	6.55(-2)
3p3d	^3F	4	691.81	2.83(-1)
	^3F	3	687.59	2.96(-1)
	^3F	2	683.76	2.37(-1)
	^3D	3	730.43	3.29(-2)
	^3D	2	726.17	3.74(-2)
	^3D	1	726.21	3.37(-2)
	^3P	2	731.76	3.76(-2)
	^3P	1	732.07	4.00(-2)
	^3P	0	732.14	4.19(-2)
	^1F	3	794.66	2.84(-2)
	^1D	2	692.51	7.56(-2)
	^1P	1	800.30	2.86(-2)

*Figures in parentheses are the power of 10 by which the preceding number should be multiplied.

Table 10 Calculated reduced electric dipole radial integrals (in atomic units) in Ti XI.

Transition		Reduced E1 integral
$3s^2$	- 3s3p	(3s:R1:3p)= 0.8651
3s3p	- $3p^2$	(3s:R1:3p)=-0.8651
	- 3s3d	(3p:R1:3d)=-1.1504
$3p^2$	- 3p3d	(3p:R1:3d)= 1.1534
3s3d	- 3p3d	(3s:R1:3p)= 0.8651

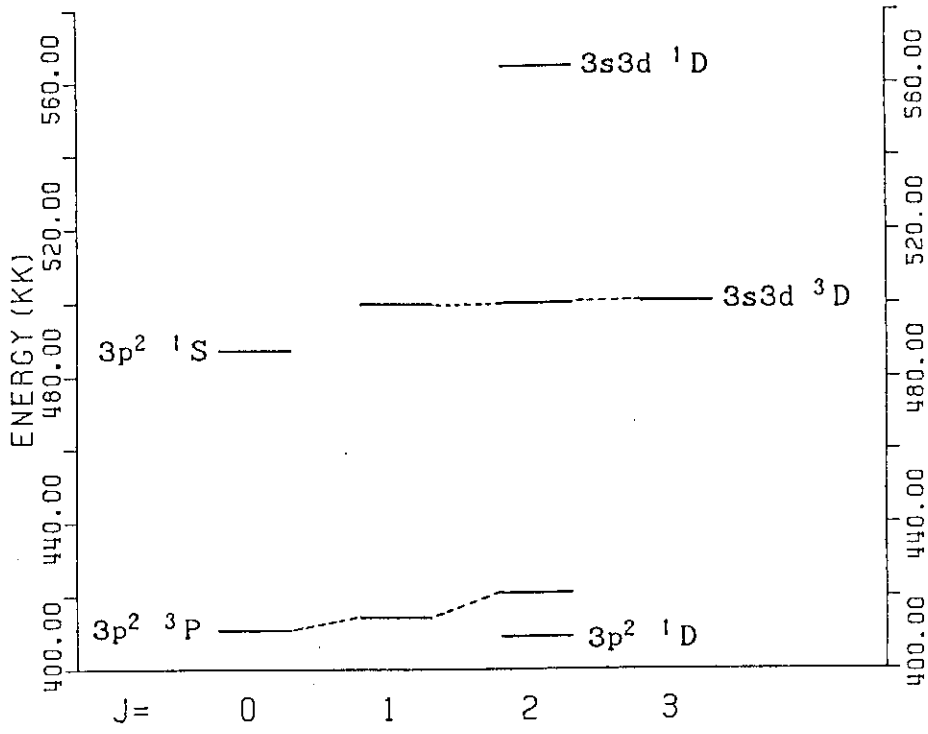

Fig.1 Calculated energy level diagram of $3p^2$ (ℝ) and 3s3d(ℂ) configurations of the first parity in Ti XI. Energy is in $10^3\,cm^{-1}$.

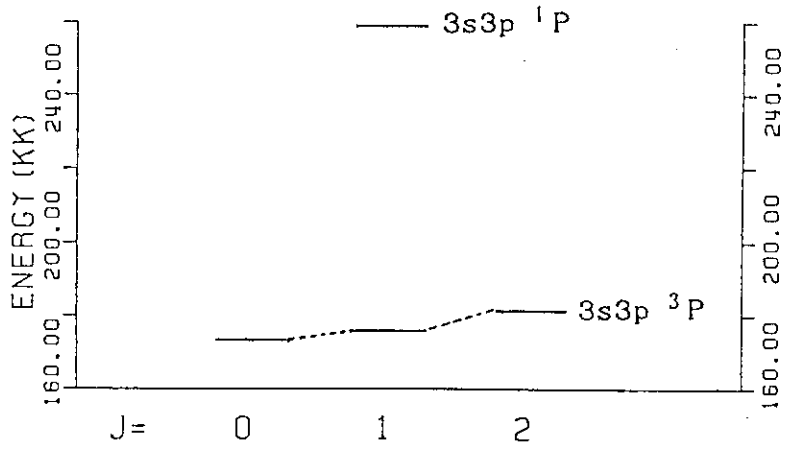

Fig.2 Calculated energy level diagram of 3s3p configuration of the second parity in Ti XI. Energy in $10^3\,cm^{-1}$.

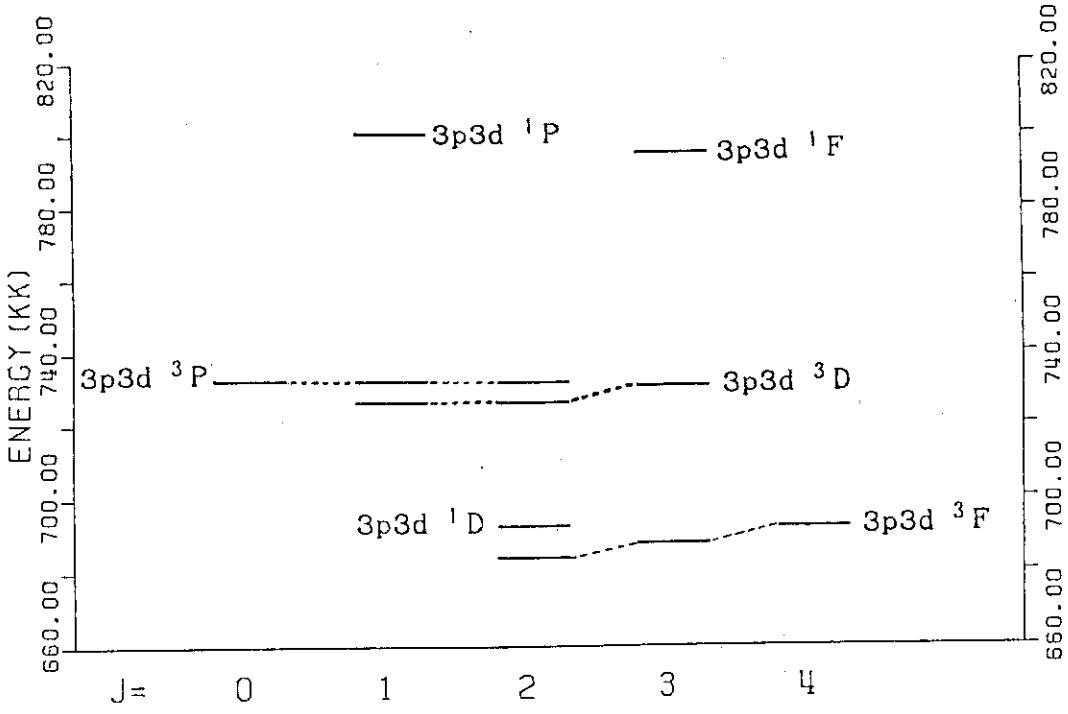

Fig.3 Calculated energy level diagram of 3p3d configuration of the the second parity in Ti XI. Energy in $10^3 cm^{-1}$.

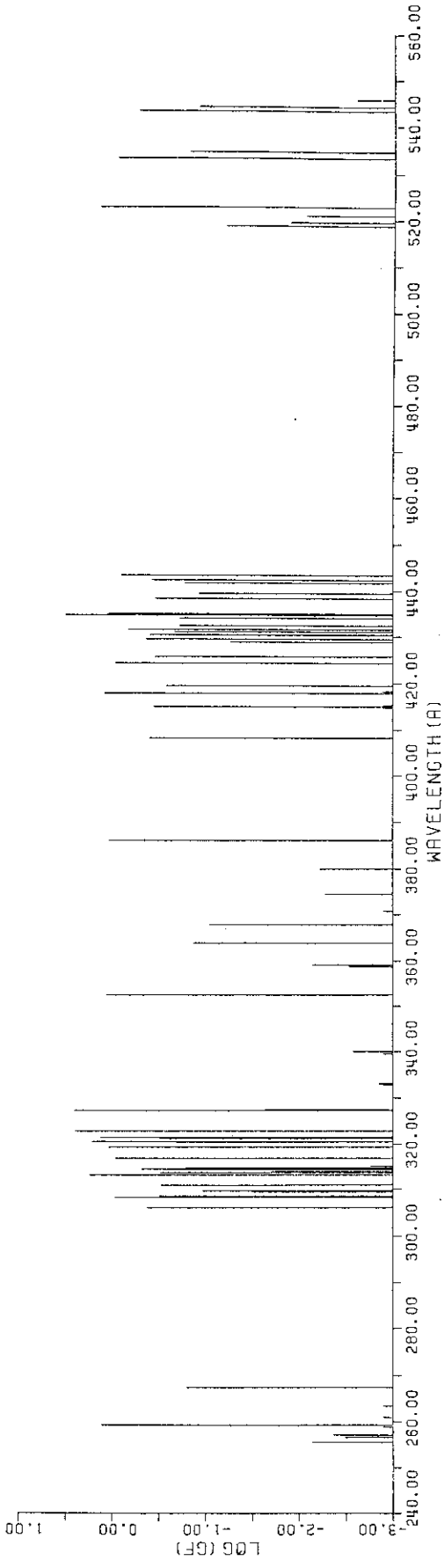

Fig.4 Calculated line pattern for the transitions in Ti XI, reproduced from Table 8.

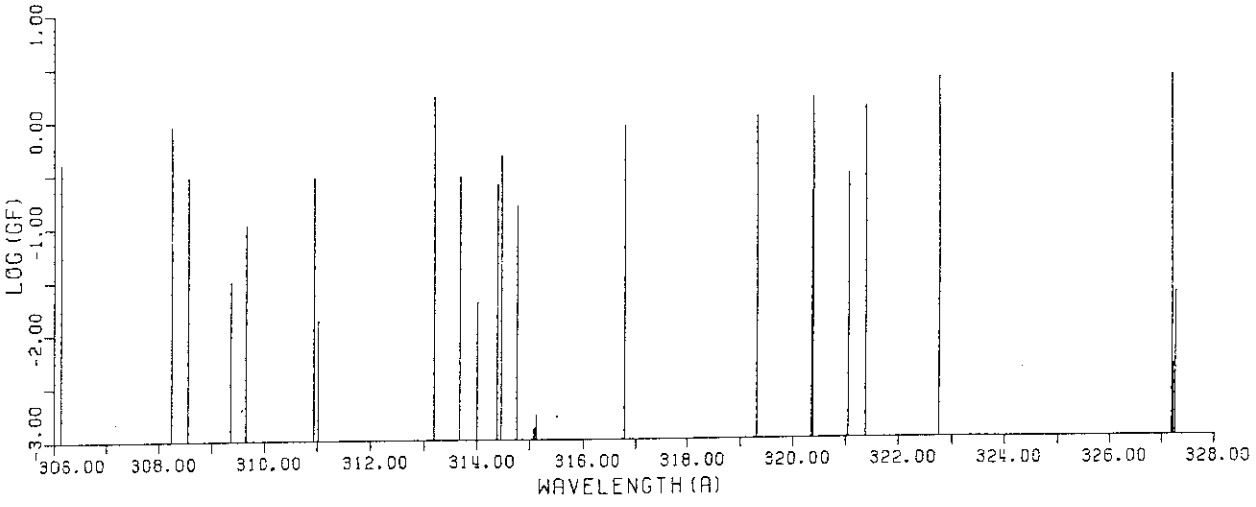

Fig.5 Calculated partial line pattern in the range from 308 to 324 Å with expanded wavelength scale.

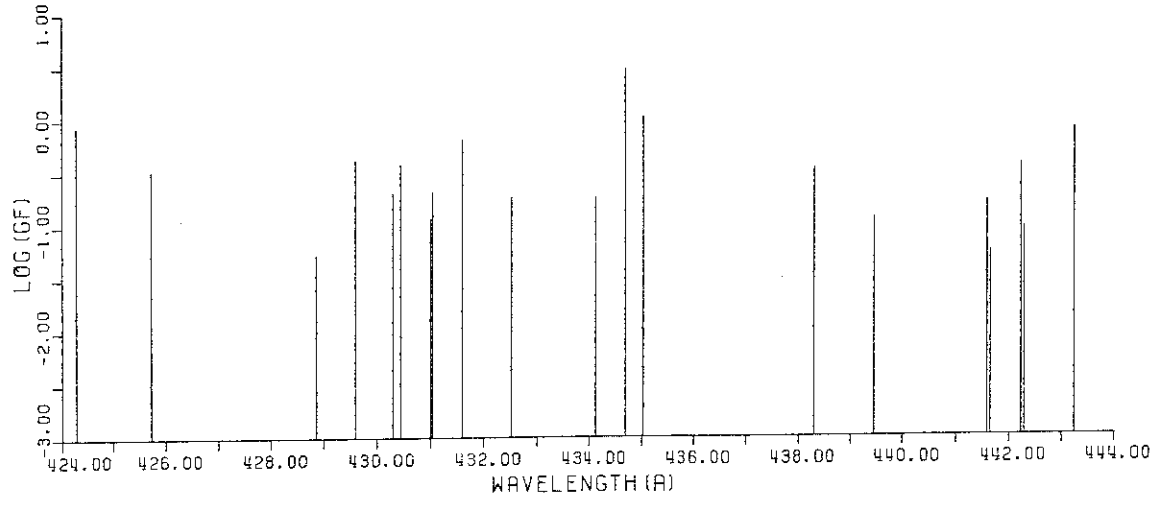

Fig.6 Calculated partial line pattern in the range from 428 to 444 Å with expanded wavelenght scale.

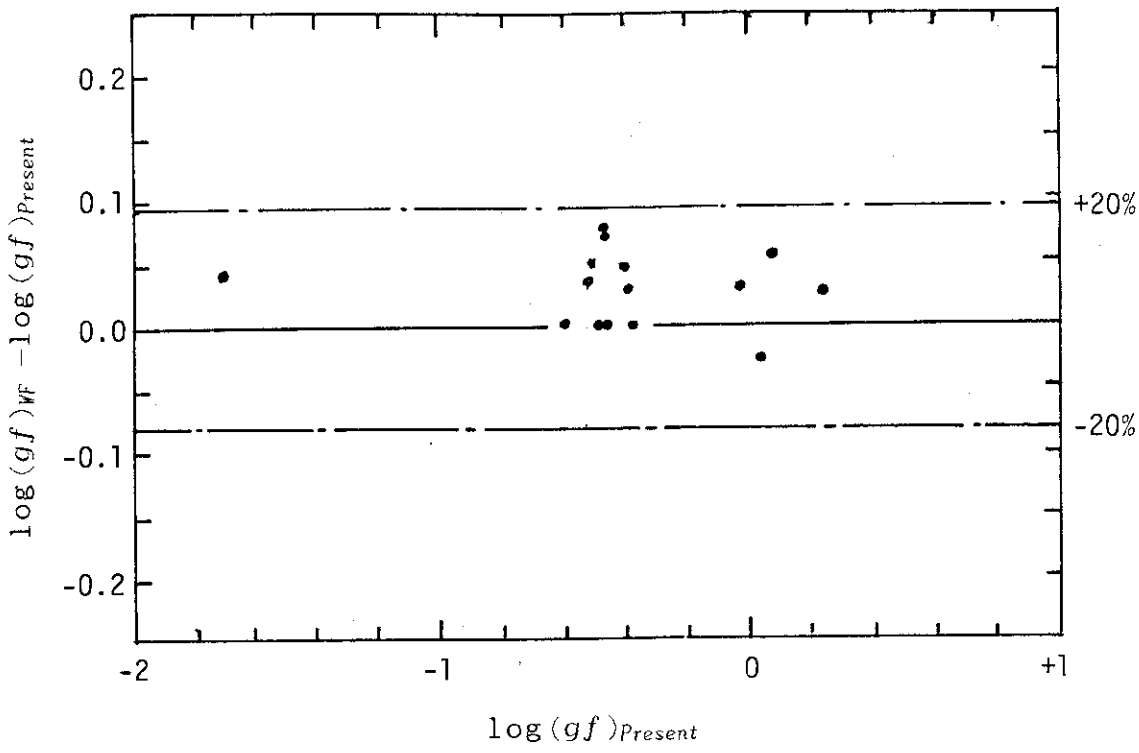

Fig.7 Plot of $\log(gf)_{WF}-\log(gf)_{Present}$ vs. $\log(gf)_{Present}$.
The are between two dashed lines indicates agreement within ±20%.